High-NA Confocal Measurement by Diffractive Optical Elements

Zheng Li

Vision and Fusion Laboratory
Institute for Anthropomatics
Karlsruhe Institute of Technology (KIT), Germany
zheng.li@kit.edu

Technical Report IES-2019-11

Abstract

Diffractive optical elements (DOEs) can produce high-numerical-aperture (NA) spots over a large field. They can be combined with a low-NA objective to measure a large area with high resolution. This work shows experiments of using DOEs in reflection confocal microscope to resolve small structures beyond the capability of the objective. Both qualitative and quantitative results have shown enhancement in lateral and axial resolution by the application of the DOEs, which also agrees to the imaging theory of confocal microscopes.

1 Introduction

Confocal microscopy has been widely used as a standard measurement method in many fields for years [11]. The resolution of a confocal microscope is mainly dependent on the numerical aperture (NA) of the objective. Objectives with higher NAs can produce smaller illumination spots, and thus they can image the sample with high resolution. However, high-NA objectives are very limited

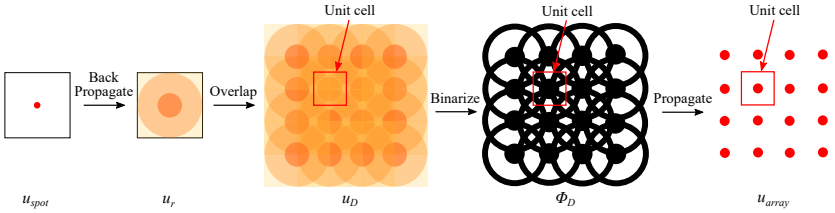

Figure 1.1: Design procedures of the DOE which generates spot array with overlapping apertures [4].

in the field of view and only a small portion of the sample can be measured at a time. Besides, high-NA objectives are also expensive due to complicated optical design and manufacture.

In order to solve the problems, diffractive optical elements are proposed to be used in confocal microscopes [3, 7, 6]. They can produce spots with overlapping apertures. Unlike the microlens array, the NA for a produced single spot is no longer limited by the unit area above it. In contrary, the surrounding area also contributes to the spot. So the proposed DOEs can produce a dense spot array with a high NA. The design procedures if the DOEs are described by Fig. 1.1 [5]. First, a required target spot field distribution u_{spot} is defined. By simulation, the target field propagates back and forms a spherical-wave-like field distribution u_r. Rayleigh-Sommerfeld integral [8, 9, 10] is used as the simulation method for the diffraction field propagation, which is shown as

$$u_r = \iint_{\Sigma} u_{spot}(\mathbf{r}') \frac{e^{-ik|\mathbf{r}-\mathbf{r}'|}z}{|\mathbf{r}-\mathbf{r}'|^2} dx'dy', \tag{1.1}$$

where Σ denotes the surface on the boundary, i.e. the plane which u_{spot} lies on and the semi-infinite sphere behind it, $\mathbf{r} = (x, y, z)$ is the coordinate of u_r, $\mathbf{r'} = (x', y', z')$ is the coordinate on Σ, and k is the wave number.

By utilizing the idea of overlapping aperture, u_r is duplicated and overlapped with a designed pitch to form the overlapping field u_D. Then the phase of u_D is extracted and binarized with a binarization factor B [3] as follows,

$$\phi_D(x, y) = \mod\left(\left\lfloor \frac{\arg[u_D(x, y)] + B}{\pi} \right\rfloor, 2\right)\pi. \tag{1.2}$$

Finally the binarized field propagates back by simulation to validate the design result. In this case, a dense spot array with a high NA can be generated by plane wave illumination. And the produced spots with an NA up to 0.77 has been demonstrated [5]. However, when being used in a confocal setup like Fig. 1.2, such DOEs introduce significant disturbances in the imaging path. In order to realize the setup, the DOEs need modification to increase the zero-order diffraction which allows the generated spots to be imaged through itself. This is done by adding a plane-wave component to the overlapped field u_D,

$$u'_D = u_D + W, \tag{1.3}$$

where W is a constant which is optimized iteratively to achieve the best signal-to-noise ratio of the spots in the image. In this way, the disturbance added by the DOE is significantly reduced when the spots are imaged through it, which has already been demonstrated by experiments [5]. The resulting DOE, which is called See-through DOE, can thus be used in the confocal microscope in Fig. 1.2. And both lateral and axial resolution can be enhanced as shown by theory and experiments in the following chapters.

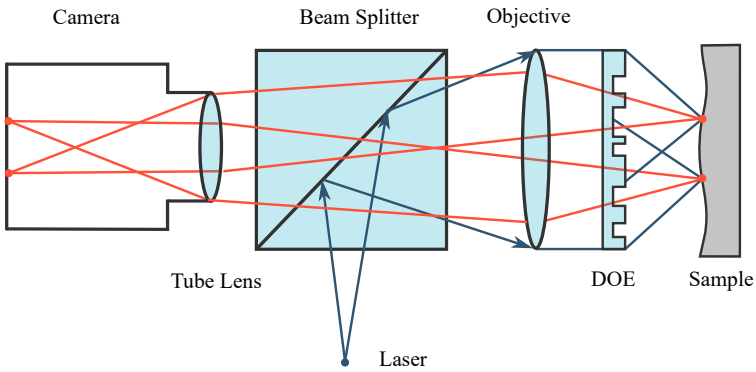

Figure 1.2: Setup of a confocal microscope using the DOE. A laser is collimated by the objective to illuminate the DOE. The produced spots are again imaged by the objective onto the camera sensor.

2 Resolution enhancement by the DOE

The confocal microscope setup in Fig. 1.2 uses a low-NA objective to increase the field of view and a see-through DOE to project high-NA spots. The objective also acts as a collimator to produce plane-wave illumination for the DOE. It is suitable for both opaque surface measurement and fluorescence microscopy, which transmission microscopes cannot measure. When an opaque surface is measured, lateral resolution can be significantly increased by the DOE while axial resolution can only be slightly increased [4]. When fluorescent samples in transparent medium are measured, both lateral and axial resolutions can be increased which is comparable to a high-NA objective.

2.1 Theory of scanning microscopy

The image formation of a scanning microscope can be described as the following equation[12]:

$$U(x_2, y_2; x_s, y_s) \tag{2.1}$$

$$= \iint_{-\infty}^{\infty} h_1(x_0, y_0) t(x_0 - x_s, y_0 - y_s) h_2\left(\frac{x_2}{M} - x_0, \frac{y_2}{M} - y_0\right) dx_0 dy_0, \tag{2.2}$$

where (x_0, y_0) is the object coordinate, (x_2, y_2) is the image coordinate, (x_s, y_s) is the scanning position, $h_1(x_s, y_s)$ is the illumination point spread function (PSF), $h_2(x_s, y_s)$ is the imaging PSF, and $t(x_0, y_0)$ is the object transmissivity or reflectivity. For a confocal microscope, a point detector is used at $x_2 = y2 = 0$ and the intensity at every scanning position can be expressed by

$$I(x_s, y_s) = \left| \iint_{-\infty}^{\infty} h_1(x_0, y_0) t(x_0 - x_s, y_0 - y_s) h_2\left(-x_0, -y_0\right) dx_0 dy_0 \right|^2, \tag{2.3}$$

which can be simplified to the following equation because the PSF is even,

$$I(x_s, y_s) = \left| h_1 h_2 * t \right|^2, \tag{2.4}$$

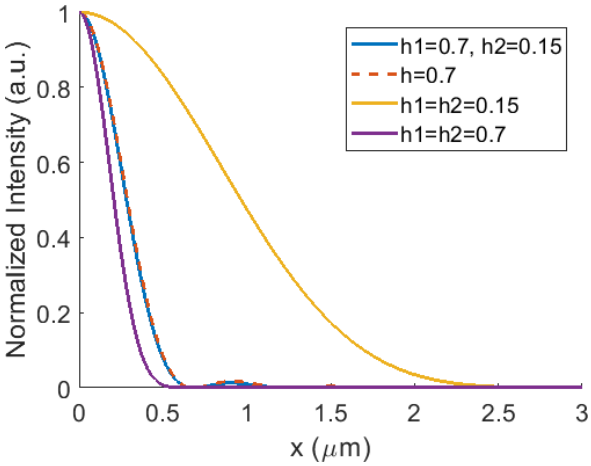

Figure 2.1: Simulation of a single point with different illumination and imaging PSFs. The dashed line represent a wide-field microscope configuration with a single PSF.

The equivalent PSF for the confocal image thus becomes $h_1 h_2$. In this case, if the illumination h_1 is high-NA and the imaging h_2 is low-NA, the combined PSF will still be dominated by the high-NA illumination.

Figure 2.1 shows the simulation results of the lateral intensity profile when a single point is imaged by illumination and imaging with different NAs. It is shown that when the illumination has high NA, the combined confocal PSF is independent of the low-NA imaging objective and is slightly smaller than the wide-field high-NA curve. Thus the lateral resolution can be increased by such a setup in Fig. 1.2. This is also very similar to the principle of super-resolution microscopy like STED [2] or PALM [1]. Similarly, the axial resolution can also be increased for a point-like object in fluorescence microscopy, which has been explained in [4].

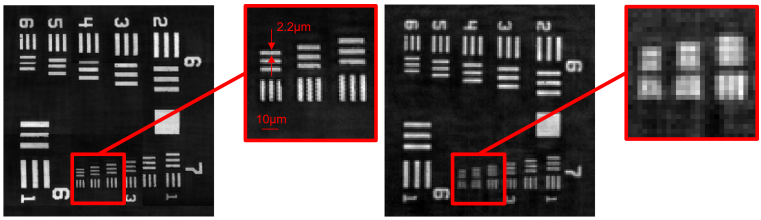

(a) DOE confocal scanning image. (b) Wide-field image.

Figure 2.2: Images of a resolution target taken by an objective with NA=0.15.

2.2 Experiments of the DOE in confocal microscopy

Experiments are also made to test the resolution enhancement by the DOE in a confocal microscope as shown in Fig. 1.2. A standard positive USAF resolution target from Thorlabs is used as the test object with a maximum resolution of 228 line pairs per millimeter. The target is scanned laterally in a zig-zag way and a confocal scanning image is obtained.

Fig. 2.2 shows a comparison of a DOE confocal scanning image and a wide-field image both taken by an objective with NA=0.15. It is obvious that the DOE increases the lateral resolution and the even finest patterns can be clearly resolved. The zig-zag like artifacts in the image are caused by insufficient accuracy of the xy stages which leads to the misalignment in the confocal image reconstruction. Contrarily, the wide-field image is totally blurred because the numerical aperture of the objective is not high enough.

Furthermore, images shown in Fig. 2.3 are also taken by an objective with an even smaller NA of 0.07. There is still a very obvious resolution enhancement. However, the signal-to-noise ratio and the resolution of the confocal scanning image are also slightly reduced compared to the image taken by an objective with an NA of 0.15.

There could be several reasons for this. First, the diffraction efficiency of a binary DOE is limited. There is unavoidable -1 order diffraction which is stray light and will be collected by the objective to form a noisy background. When

the NA of the objective is lower, the signal is weaker so the signal-to-noise ratio is reduced. This phenomenon can be mitigated by using a multi-level DOE to increase the diffraction efficiency. Moreover, the Andor Zyla 5.5 camera we used has a large pixel size of $6.5\,\mu\mathrm{m}$. And we use a $0.63\times$ tube lens and a $2.5\times$ objective with NA=0.07. The total magnification is 1.575, which is pretty small. This leads to a relatively large equivalent pinhole size of roughly $3.7\,\mu\mathrm{m}$, which cannot effectively block the stray light. By using a camera with a smaller pixel size or a tube lens with a larger magnification can mitigate the problem.

After the lateral measurement, the axial resolution is also tested with the fluorescence microscope setup shown in Fig. 2.4. The Sphero Rainbow fluorescent particles are used as samples. The excitation wavelength is $630\,\mathrm{nm}$ and the emission wavelength is from $672\,\mathrm{nm}$ to $712\,\mathrm{nm}$. The sizes of the beads are 3.0-$3.4\,\mu\mathrm{m}$. In the experiment, only one fluorescence bead is focused. The bead is moved vertically to measure the intensity response. Both objectives with NA of 0.15 and 0.07 are used for testing. The produced spots have axial full width at half maximum (FWHM) of $19.5\,\mu\mathrm{m}$ and $17.2\,\mu\mathrm{m}$ respectively, which corresponds to a NA of roughly 0.25, because of the different collimation quality of the objectives. The confocal signals show axial FWHM of $25.9\,\mu\mathrm{m}$ and $26.3\,\mu\mathrm{m}$ respectively. The results show that the axial resolution is almost independent on the imaging objective, which is predicted by the theory. Still the confocal axial peaks are a bit wider than the illumination spot. The reason can be that the pixel as a pinhole is large, and the diameter of the bead is not negligible.

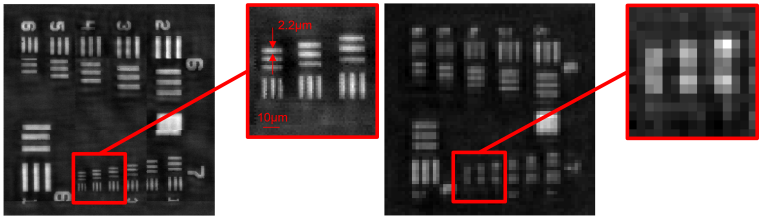

(a) DOE confocal scanning image. (b) Wide-field image.

Figure 2.3: Images of a resolution target taken by an objective with NA=0.07.

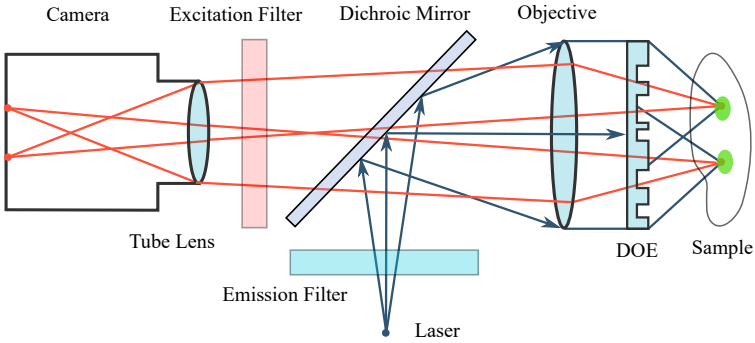

Figure 2.4: Setup of a fluorescence confocal microscope using the DOE.

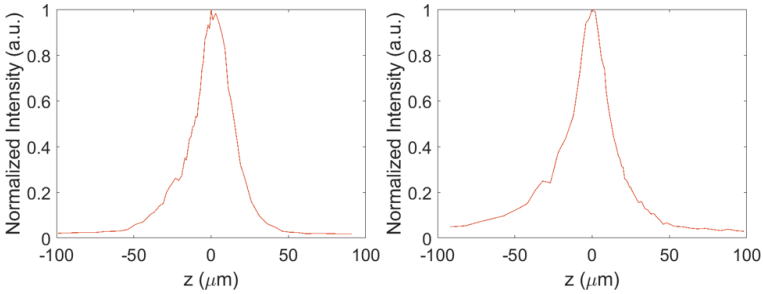

(a) Axial response by an objective with NA=0.15.

(b) Axial response by an objective with NA=0.07.

Figure 2.5: Axial intensity response of an in-focus fluorescent bead.

3 Conclusion

Traditional confocal microscopy relies on high-NA objectives to achieve high resolution. However, high-NA lenses have a very limited field of view. The See-through DOE can be used with a low-NA objective in a reflection confocal microscope to provide a large field of view. The DOE can produce high-NA spots and maintain the resolution of a high-NA objective in such a setup.

For surface measurements, 2D scan was performed and the enhancement of resolution is clearly demonstrated. Meanwhile, the See-through DOE is also successfully used in fluorescence microscopy. Fluorescence signals of the beads were observed and also axial response was tested. The axial FWHMs are independent of the NA of the objective, which also agrees with the theory.

In the future, for surface measurement, the measurement uncertainty will be tested. For fluorescence measurement, a 3D scan of living cells will be carried out. New experiments are planned to further demonstrate the capability of the DOEs to increase the measurement resolution.

References

[1] Eric Betzig et al. “Imaging intracellular fluorescent proteins at nanometer resolution”. In: *Science* 313.5793 (2006), pp. 1642–1645.

[2] Stefan W Hell and Jan Wichmann. “Breaking the diffraction resolution limit by stimulated emission: stimulated-emission-depletion fluorescence microscopy”. In: *Optics letters* 19.11 (1994), pp. 780–782.

[3] Bas Hulsken, Dirk Vossen, and Sjoerd Stallinga. “High NA diffractive array illuminators and application in a multi-spot scanning microscope”. In: *Journal of the European Optical Society - Rapid publications* 7 (2012).

[4] Zheng Li. “Application of diffractive optical elements in confocal microscopy”. In: *Proceedings of the 2018 Joint Workshop of Fraunhofer IOSB and Institute for Anthropomatics, Vision and Fusion Laboratory. Ed.: J. Beyerer, M. Taphanel*. Vol. 40. Karlsruher Schriften zur Anthropomatik / Lehrstuhl für Interaktive Echtzeitsysteme, Karlsruher Institut für Technologie ; Fraunhofer-Inst. für Optronik, Systemtechnik und Bildauswertung IOSB Karlsruhe. KIT Scientific Publishing, Karlsruhe, 2019, pp. 25–46. ISBN: 978-3-7315-0936-3.

[5] Zheng Li et al. “Application of DOE in confocal microscopy for surface measurement”. In: *Photonics and Education in Measurement Science 2019*. Ed. by Maik Rosenberger, Paul-Gerald Dittrich, and Bernhard Zagar. Vol. 11144. International Society for Optics and Photonics. SPIE, 2019, pp. 254–261. DOI: 10.1117/12.2531610. URL: https://doi.org/10.1117/12.2531610.

[6] Xiyuan Liu and Karl-Heinz Brenner. “High Resolution Wavefront Measurement with Phase Retrieval Using a Diffractive Overlapping Micro Lens Array”. In: *Fringe 2013*. Springer, 2014, pp. 233–236.

[7] Xiyuan Liu, Tim Stenau, and Karl-Heinz Brenner. “Diffractive micro lens arrays with overlapping apertures”. In: *Information Optics (WIO), 2012 11th Euro-American Workshop on*. IEEE. 2012, pp. 1–2.

[8] Fabin Shen and Anbo Wang. “Fast-Fourier-transform based numerical integration method for the Rayleigh-Sommerfeld diffraction formula”. In: *Applied optics* 45.6 (2006), pp. 1102–1110.

[9] Arnold Sommerfeld. *Mathematical Theory of Diffraction*. Boston, MA: Birkhäuser Boston, 2004, pp. 9–68. ISBN: 978-0-8176-8196-8. DOI: 10.1007/978-0-8176-8196-8_2. URL: https://doi.org/10.1007/978-0-8176-8196-8_2.

[10] Arnold Sommerfeld. “Mathematische theorie der diffraction”. In: *Mathematische Annalen* 47.2 (1896), pp. 317–374.

[11] Jeroen Vangindertael et al. “Super-resolution mapping of glutamate receptors in C. elegans by confocal correlated PALM”. In: *Scientific reports* 5 (2015), p. 13532.

[12] Tony Wilson and Colin Sheppard. *Theory and practice of scanning optical microscopy*. Vol. 180. Academic Press London, 1984.